

Analysis of inhomogeneous optical systems by the use of ray tracing. I. Planar systems

Gleb Beliakov and D. Y. C. Chan

We describe a novel approach to refractive-index reconstruction in two-dimensional systems with no special symmetry, based on observation of traces of rays that travel through the optical system. The mathematical model of ray-tracing analysis is presented in detail, and both the analytical and numerical solutions are given. Methods of data processing in the presence of experimental errors are developed and applied to model problems. © 1997 Optical Society of America

Key words: Refractive-index distribution, ray-tracing, gradient-index lens, nondestructive diagnostics.

1. Introduction

The problem of reconstructing refractive-index distribution of inhomogeneous optical media arises in many areas of research, such as optical fiber profiling,¹⁻⁵ diagnostics of planar waveguides,^{6,7} plasma diagnostics, and analysis of crystalline lenses.⁸ In the case in which the analyzed system possesses circular or elliptic symmetry, the problem is well studied, and the methods of solution are based on the transformation of the measured optical path^{1,2,4,9} or the deflection angle^{5,8,10} into the refractive-index profile. For the systems without symmetry, several methods based on computer tomography^{10,11} and spherical aberrations¹² have been reported. In this paper we present a novel, highly precise approach to the problem of nondestructive diagnostics of asymmetric objects, which is based on observation of the traces of thin coplanar laser beams (rays) that travel through the optical system. We call this method the ray-tracing analysis.

In ray-tracing experiments, a set of rays is passed through a region for which the refractive index is to be found (Fig. 1). We refer to this set of rays as sampling rays. The traces of the sampling rays are visible because of scattering and can be registered and digitized. The positions of the points that form

sampling rays are then used to compute the distribution of the refractive index by the mathematical methods described below.

Ray-tracing analysis has been applied to nondestructive diagnostics of planar waveguides.^{6,7} It can also be applied to the analysis of three-dimensional optical systems with cylindrical symmetry, for which the refractive index varies with the spatial coordinates (x, y, z) such as $n = n(r, z)$, $r^2 = x^2 + y^2$. For such systems the variation of the index is essentially a two-dimensional problem.

Unlike some other methods, an advantage of the ray-tracing analysis is that it does not assume any particular model of the refractive index. However, the numerical problem of determining index distribution from measured ray path data is ill-conditioned, and the result can be sensitive to noise in the data. In this paper we present methods both to regularize the problem and to obtain a quantitative indication of the level of experimental accuracy that would be required for the ray-tracing data to achieve a given desired accuracy in the refractive index.

2. Mathematical Model

In terms of geometric optics, the propagation of light in an optical media is described by the eikonal equation¹³

$$[\nabla S(\mathbf{r})]^2 = n(\mathbf{r})^2, \quad (1)$$

where $S(\mathbf{r})$ denotes the optical path and $n(\mathbf{r})$ is the refractive index in a point $\mathbf{r} = (x, y, z)$. The function $S(\mathbf{r})$ is called the eikonal. The surfaces $S(\mathbf{r}) = \text{const}$ are called the wave fronts.

The geometric light rays may be defined as the orthogonal trajectories to the wave fronts. They are

The authors are with the Department of Mathematics and Statistics, The University of Melbourne, Parkville, VIC 3052, Australia.

Received 20 February 1996; revised manuscript received 31 July 1996.

0003-6935/97/225303-07\$10.00/0

© 1997 Optical Society of America

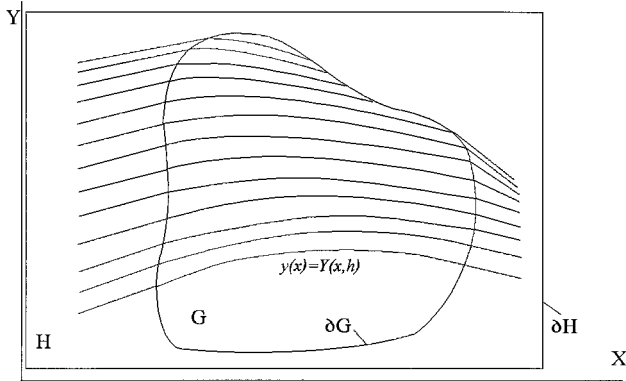


Fig. 1. Ray paths through an optical system.

regarded as oriented curves whose direction coincides everywhere with the direction of the average Poynting vector (for isotropic media¹³). The position vector \mathbf{r} of a point on the ray path satisfies the ray equation

$$\frac{d}{ds} \left(n \frac{d\mathbf{r}}{ds} \right) = \nabla n, \quad (2)$$

where ds denotes an element of the ray path. When $n(\mathbf{r})$ is not continuous, Snell's law $n(\mathbf{r}_1) \sin \theta_1 = n(\mathbf{r}_2) \sin \theta_2$ is used in conjunction with the locality principle¹⁴: namely that reflection and refraction proceed in such a manner as if the incident wave were plane and the curvilinear boundary were replaced by a tangent plane at the point of incident. Here θ_1 and θ_2 are the angles that the incident and refracted rays make with the normal to the tangent plane.

Consider a two-dimensional inhomogeneous optical medium with smooth refractive index $n = n(x, y)$. We assume that the rays $\mathbf{r}(s) = [x(s), y(s)]$ allow the unique parameterization $y = y(x)$, which is valid for modest variations of n . With this assumption, Eq. (2) can be rewritten (see Appendix) as

$$-y' \frac{\partial w}{\partial x} + \frac{\partial w}{\partial y} - \frac{y''}{1 + (y')^2} = 0, \quad (3)$$

where $w(x, y) = \ln[n(x, y)]$.

Using Eq. (3) two problems may be formulated: the direct and the inverse problem. In the direct problem the refractive index is given, and Eq. (3) determines the rays $y = y(x)$ that would travel through such an optical medium. This problem is also known as the problem of ray tracing, and fast and accurate methods of its solution are given elsewhere (see, e.g., Ref. 15 and references therein).

The inverse problem can be studied as follows: Suppose one observes a family of sampling rays, parameterized by h ,

$$\{y(x) = Y(x, h), h_- \leq h \leq h_+\}, \quad (4)$$

which covers a planar area G with unknown refractive index, such as in Fig. 1. The problem is to determine the refractive index $n(x, y)$ by use of this information.

Provided that the function $Y(x, h)$ satisfies the following conditions, the solution for $n(x, y)$ exists:

- (1) $Y(x, h)$ has continuous second partial derivatives $Y_{xx}(x, h)$.
- (2) $Y(x, h)$ has continuous first partial derivatives $Y_h(x, h)$ and $Y_h(x, h) \neq 0$ in G .
- (3) $Y(x, h)$ has continuous second mixed partial derivatives $Y_{xh}(x, h)$.

We defer the discussion of uniqueness of the solution.

The first and the third conditions that guarantee the existence of the solution imply that $Y(x, h)$ is a sufficiently smooth function, while the second condition implies that the sampling rays cover all G and, very important, do not intersect in G . That is, the equation $h = h(x, y)$ has a unique solution for every $(x, y) \in G$.

It is convenient to rewrite Eq. (3) in the following form:

$$C(x, y) \frac{\partial w}{\partial x} + \frac{\partial w}{\partial y} = F(x, y), \quad (5)$$

where

$$C(x, y) = -Y_x(x, y)|_{h=h(x, y)},$$

$$F(x, y) = \frac{Y_{xx}(x, y)}{1 + Y_x^2(x, y)}|_{h=h(x, y)}. \quad (6)$$

Equation (5) is equivalent to the following system of ordinary differential equations, whose solutions are called characteristics of Eq. (5):

$$\begin{cases} \frac{dx}{dy} = C(x, y), & (7a) \\ \frac{dw}{dy} = F(x, y). & (7b) \end{cases}$$

The characteristics have a direct physical interpretation: The solutions of the first equation $x = x(y)$ determine the wave fronts (the curves orthogonal to the rays), and the second equation determines the refractive index on the wave fronts. Thus, the inverse problem can be solved by solving the system of ordinary differential equations [Eqs. 7(a) and 7(b)] with initial conditions to be given below.

3. Analytical Solution

The analytical solution for the inverse problem was first given in a series of papers in Russian by Mikaelian (see Ref. 16). We briefly present the results. According to Ref. 16, the general analytical solution of the inverse problem for a large class of ray families can be reduced to a calculation of integrals. Let the function $h(x, y)$ be given by a product of functions $g(x)$ and $f(y)$: $h(x, y) = g(x)f(y)$.

Then from Eqs. (6) and (7) we have

$$\frac{dy}{dx} = -\frac{g'(x)f(y)}{g(x)f'(y)},$$

which can be integrated by a separation of variables to give

$$\int \frac{g(x)}{g'(x)} dx = -\int \frac{f(y)}{f'(y)} dy + C_1, \quad (8)$$

where C_1 is an arbitrary constant. Denote by S the sum of both integrals. The first solution of the system [Eqs. (7)] may be written in the form $S(x, y) = C_1$, and $S(x, y)$ is therefore a wave front.

Let $x = X(y, C_1)$ be the solution of Eq. (7a). Then Eq. (7b) can be integrated:

$$\begin{aligned} w(x, y) &= \ln[n(x, y)] \\ &= \int F[X(y, C_1), y] dy \Big|_{C_1=S(x, y)} + C_2. \end{aligned} \quad (9)$$

The general solution may be written in the form $T(C_1, C_2) = 0$, and the refractive index $n(x, y)$ is given explicitly by

$$\begin{aligned} n(x, y) &= \exp\left\{ \int F[X(y, C_1), y] dy \Big|_{C_1=S(x, y)} \right. \\ &\quad \left. + \Phi[S(x, y)] \right\}, \end{aligned} \quad (10)$$

where $\Phi[S(x, y)]$ is an arbitrary function.

A particular consequence of Eq. (10) is that the ray traces do not determine the refractive index uniquely but up to an arbitrary function of wave fronts. Therefore, if the solution to the inverse problem exists, the problem has infinitely many solutions.

The latter statement is also valid for an arbitrary family of rays, according to the principle of inhomogeneous media similarity.¹⁶ Consider inhomogeneous optical media with $n_1 = n_1(\mathbf{r})$. The wave fronts are given by the equation $S(\mathbf{r}) = \text{const}$. The wave fronts would remain the same if we write the former equation in the form $\phi[S(\mathbf{r})] = \text{const}$, with ϕ being an arbitrary C^1 function with monotone growth. Substituting $S(\mathbf{r})$ in the eikonal Eq. (1), we have

$$\phi'[S(\mathbf{r})][\nabla S(\mathbf{r})^2]^{1/2} = n(\mathbf{r}).$$

Denote $\phi'[S(\mathbf{r})]$ by $\Phi[S(\mathbf{r})]$. The former equation now takes the form $n(\mathbf{r}) = n_1(\mathbf{r})\Phi[S(\mathbf{r})]$, where $\Phi > 0$ is an arbitrary function. Consequently, the rays [Eq. (4)] determine the refractive index up to an arbitrary function of wave fronts.

The reason we obtained infinitely many solutions is that on a given wave front the refractive index may be determined up to an arbitrary constant C . For every wave front this constant is different, so that the solution on one wave front does not depend on the solution on another wave front. Suppose now that on

a wave front $S(x, y) = C_1$ there is one point at which the refractive index is known. Then the refractive index on this wave front is determined uniquely, which follows from the uniqueness of the solution for ordinary differential equations. If every wave front in G contains exactly one point with a given refractive index, $n(x, y)$ is determined uniquely in G . In practice, the index is known on the boundary of region G .

As a specific example, consider a family of ray paths given by $h(x, y) = \sin h(y)/\sin(x)$. Equation (8) yields the following equation for wave fronts:

$$S(x, y) = \frac{\cosh(y)}{\cos(x)} = C_1.$$

The function $F(x, y)$ in Eq. (7b) may be obtained from

$$\frac{d^2 h(x, y)}{dx^2} = 0,$$

which gives

$$F(x, y) = -\tanh(y).$$

Now the general solution of the system [Eqs. (7)] can be written in the form

$$n(x, y) = \frac{1}{\cosh(y)} \Phi \left[\frac{\cosh(y)}{\cos(x)} \right],$$

where Φ is an arbitrary function. In particular, when n does not depend on x , it corresponds to a well-known solution for the Selfoc waveguides,

$$n(y) = \frac{n(0)}{\cosh(y)},$$

also called the Mikaelian lens.¹⁶

Consider now an optical medium whose refractive index is piecewise smooth. The simplest example of such a system is an optical medium G with a smooth refractive index placed into another medium H whose refractive index is also smooth (Fig. 1). It can be a thick lens in air, a crystalline lens of the eye in water, a waveguide in matching oil, and so forth. As we mentioned above, the ray traces satisfy Eq. (3) in the smooth parts of the system and Snell's law on discontinuities. Consequently, the rays are smooth in G and H but are not differentiable on the boundary ∂G . The method of ray-tracing analysis can be applied separately to G and to H provided that inside each medium conditions (1)–(3) hold and the refractive index is specified on all boundaries $\partial G \cup \partial H$. The refractive index on the boundaries can be found either by direct measurement, such as in Ref. 17, or, when the boundary is not accessible, by Snell's law. In the latter case, the index must be known in the outer part of the system, H , and so must be the slopes of the rays in H and in G near ∂G . The computation of the index in H does not require its knowledge or ∂G , but on the outmost boundary ∂H , and this can be done by direct measurement.¹⁷ No matter how many media are put one into another, the computation of the

index distribution in any of them requires the boundary condition on the outer boundary, with the outmost boundary always accessible for direct measurement.

Therefore the ray-tracing analysis of media with discontinuities is reduced to consecutive analysis of its smooth parts.

4. Numerical Solution and Treatment of Noisy Data

The experimental data are represented in digital form as a set of points on the sampling rays:

$$\begin{aligned} \{(x_{ij}, y_{ij}): y_{ij} = Y(x_{ij}, h_j), \\ i = 1, 2, \dots, N_j, \\ j = 1, 2, \dots, M\}, \end{aligned} \quad (11)$$

where x_{ij} is the abscissa of the i th point on the ray j , y_{ij} is the ordinate of this point, N_j is the number of registered points on the ray j , and M is the number of sampling rays. We also assume that the index function $w(x, y) = \ln[n(x, y)]$ is known on the boundary ∂G and that all the points in Eq. (11) belong to the interior of G .

The solution of the general problem given by Eqs. (7) is performed in two steps. In the first step the functions $C(x, y)$ and $F(x, y)$ are computed from the experimental data given by Eq. (11), and in the second step the system (7) is solved. As Eq. (7a) does not depend on w explicitly, it can be integrated separately from Eq. (7b), and this allows one to develop an efficient algorithm to compute the solution with only the values of $C(x, y)$ on the rays, that is, $C[x, Y(x, h)]$. This results in a set of points $\{y_j, X(y_j), j = 1, \dots, M\}$, which are the points of intersection of the sampling rays with a given wave front. Then the values of $F(x, y)$ are computed in these points, and Eq. (7b) may be integrated by any method of numerical integration. A precise and computationally efficient method is to interpolate the values $\{y_j, F[X(y_j), y_j]\}_{j=1}^M$ with a cubic spline and to compute $w[X(y), y]$ as the integral of the spline plus boundary conditions. This approach does not require knowledge of $C(x, y)$ and $F(x, y)$ at every point of G but only on the rays and thus has modest requirements for computer memory and speed. The integration of a cubic spline has fourth-order precision (with respect to the distance between two neighboring rays), and the wave front can be determined with second-order precision.

The method of ray-tracing analysis is stable with respect to errors in the boundary conditions. Because on the wave front $x = X(y)$ the logarithm of the refractive index is given by

$$w[X(y), y] = \int_{y_0}^y F[X(y), y] dy + w_0,$$

the error δw_0 in determining w_0 results in the same error in $w(x, y)$: $\delta w[X(y), y] = \delta w_0$. Methods for accurate determination of boundary conditions are discussed in Ref. 17.

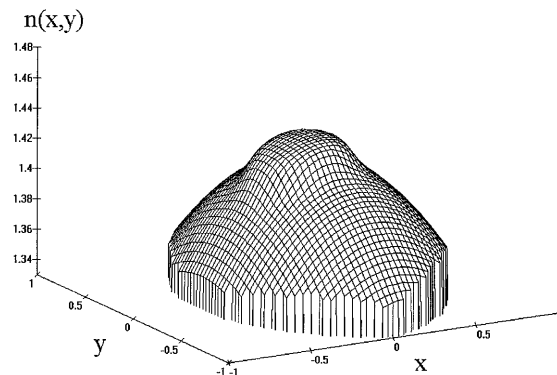


Fig. 2. Refractive index reconstructed from precise data.

Implementation of the described technique, applied to the set of 40 sampling rays with 30–100 registered points on each, results in very good agreement of the reconstructed refractive index with the model used for ray tracing. In Fig. 2 we present a plot of computed refractive index, which is virtually indistinguishable from the model used to produce the ray path data [Eq. (11)], namely,

$$\begin{aligned} n(x, y) = 1.42\{1 - 0.2[(x - 0.1)^2 + (0.7y)^2]\}^{1/2} \\ + 0.01/\cosh[200(x^2 + y^2)^2]. \end{aligned}$$

G is given by the intersection of two circles with centers in $(-0.3, 0)$ and $(0.5, 0)$, and with radii $(1 + 0.3^2)^{1/2}$ and $(1 + 0.5^2)^{1/2}$, respectively, as given in Fig. 3. The maximum error of reconstruction is 0.0024 with the average error 0.00021. Note that the chosen $n(x, y)$ has a lumpy inhomogeneous structure that may be present in ocular lenses.

Now we turn to the most difficult part of the solution: computation of $C(x, y)$ and $F(x, y)$ in Eqs. (7) from noisy experimental data. These functions are expressed in Eq. (6) through the first and the second derivatives of the measured ray path function $Y(x, h)$ given by a table of its noisy values. The problem of numerical differentiation is an ill-conditioned problem, which makes the reconstruction of the refractive index ill-conditioned as well. The regularization of

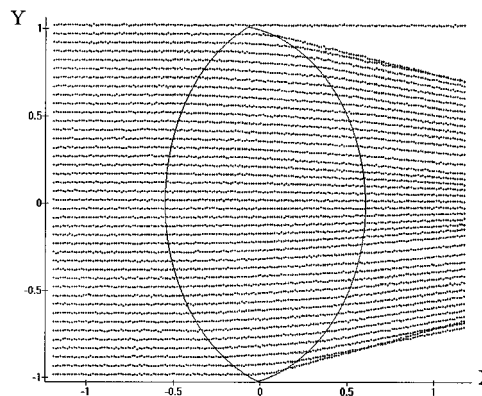


Fig. 3. Model of sampling rays: precise values plus Gaussian noise (zero mean, standard deviation $\sigma = 0.001$).

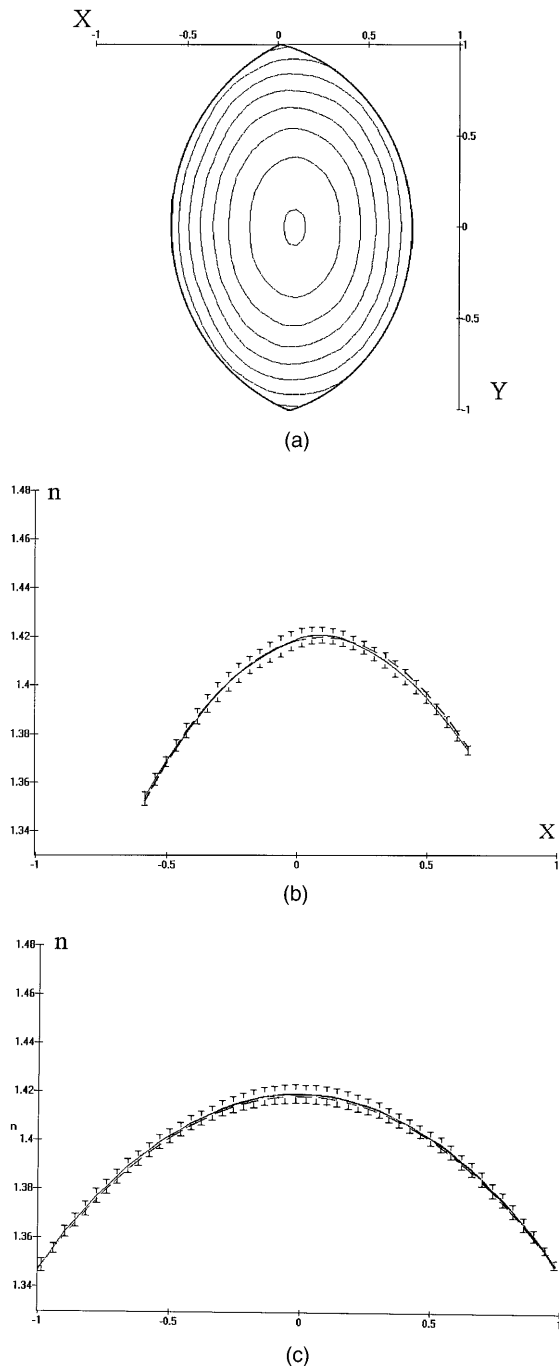


Fig. 4. Results of the refractive-index reconstruction using noisy data. (a) Contour plot of the reconstructed index, (b) section $y = 0$, (c) section $x = 0$. Reconstructed index profile is plotted in solid curves. True refractive index, given by $n(x, y) = 1.42\{1 - 0.2[(x - 0.1)^2 + (0.7y)^2]\}^{1/2}$, is plotted in dashed curves. Standard deviation of the noise, $\sigma = 0.001$; maximum error of reconstruction, 0.0028; average error, 0.00080. Confidence intervals ($p = 0.95$) are also shown.

data, inevitable for numerical differentiation, must, on the one hand, be sufficiently strong to remove the oscillations in the second derivative caused by the noise and, on the other hand, be flexible enough to characterize variations of the function $Y(x, h)$. In

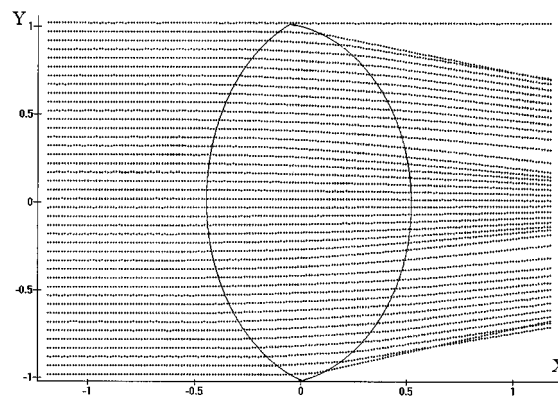


Fig. 5. Sampling rays with Gaussian noise (zero mean, standard deviation $\sigma = 0.0003$) used for reconstruction of the refractive index in Fig. 2.

Eqs. (7) we have proposed the use of constrained smoothing splines for the generalized Luneburg lens index reconstruction. This approach takes into account the specific structure of the Luneburg lens. The *a priori* knowledge that the analyzed preform is somewhat similar to the Luneburg lens allows one to impose adequate restrictions on the second derivative of the spline and thus to obtain a high-quality solution.

In general cases, when the refractive index is an arbitrary function, one may use smoothing splines without restrictions, but the price for spline flexibility is considerable loss of precision. Furthermore the traditional methods for choosing a smoothing parameter, such as the generalized cross validation and a true mean-square method,^{18,19} systematically oversmooth the solution. All these methods give splines that can hardly be distinguished from the true solution when plotted, but which fail to approximate well the second derivative. We recall that the smoothing parameter plays an important role in the theory of splines and controls the trade-off between the requirements of smoothness and the goodness of fit. Excessively large values of the smoothing parameter lead to oversmoothing while values that are too small lead to oscillations of the spline.

We have found that the best results are obtained with smoothing splines of 5th degree when the smoothing parameter p is so small that oscillations of the spline are not completely canceled. Such a selection can be done by solving

$$\|S^{(2m-2)}(x)\|_{\infty} = C,$$

where S is the spline of degree $2m-1$, which minimizes

$$p \int_a^b [S^{(m)}(x)]^2 dx + \sum_{i=1}^N [S(x_i) - y_i]^2,$$

where x_i, y_i are data points from Eq. (11) (the index j is suppressed here), p is the smoothing parameter, and C is a prescribed value. The idea is to select C

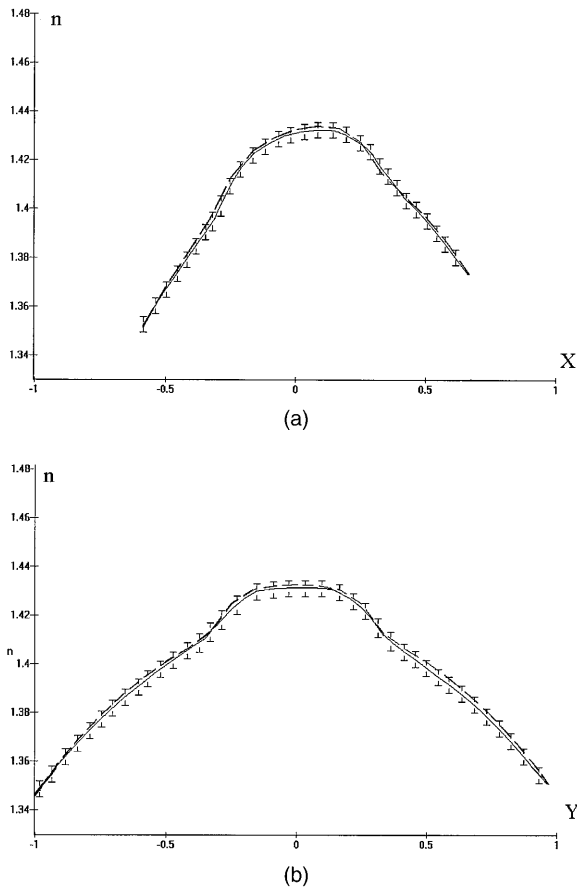


Fig. 6. Results of refractive index reconstruction (a) section $y = 0$, (b) section $x = 0$. Reconstructed index is shown by the solid curve, and the true index is shown by the dashed curve. Standard deviation of the noise, $\sigma = 0.0003$; maximum error of reconstruction, 0.0031; average error, 0.0011. The confidence intervals ($p = 0.95$) are shown.

to be slightly bigger than the estimated L_∞ – norm of the true $(2m - 2)$ th derivative of the ray and thus to prevent the spline from oversmoothing.

Because this method does not completely cancel oscillations caused by random noise in the data, the resulting refractive index also contains some randomness. The next step consequently is to perform index reconstruction with different sets of sampling rays and to average the results. This allows us to make *a posteriori* error analysis and to compute the confidence intervals for the resulting refractive index. To cancel possible systematic errors, the use of sampling rays with different initial slopes is recommended, that is, rotation of the analyzed optical system.

In Fig. 4 the results of model calculations of ray-tracing analysis are presented. First, several sets of sampling rays were obtained by ray tracing with pseudorandom Gaussian noise added to the ordinates of the points [Eq. (11)] to simulate experimental uncertainties (Fig. 3). The number σ denotes the standard deviation of the noise, and, because the units are selected in a way that the characteristic size of the

system is of an order of 1, the value $1/\sigma$ may also be interpreted as the signal-to-noise ratio.

The noisy sampling rays were used to reconstruct the refractive-index distribution. Then the refractive indices that correspond to different sets of sampling rays were averaged and compared with the refractive index used for ray tracing. It can be seen that our method correctly reconstructs the shape of the refractive index. An adequate precision can be achieved when experimental errors are sufficiently small, of an order of 0.1% of the measured values. Consequently, the readings of the positions of sampling rays must be performed with high accuracy. In this context, the finite width of sampling rays and the resolution of the measurement device may limit the attainable precision. In our simulations we selected the noise level that seems to model the actual measurement errors, and these rays are plotted in Fig. 3. For rather homogeneous refractive indices the results are most satisfactory. For reconstruction of highly inhomogeneous structures, such as in Fig. 2, additional accuracy of data is needed, because in this case the second derivative of the rays has a more complicated form. In this case, precision similar to that in Fig. 4 was obtained when the standard deviation of the noise σ was three times smaller. The ray paths used for reconstruction are shown in Fig. 5, and the results of index reconstruction are presented in Fig. 6.

5. Conclusion

The ray-tracing analysis represents a powerful alternative to the methods based on inversion of measured optical path or deflection angle. It does not require circular or elliptic symmetry of the optical system and thus is applicable to a much wider class of problems. The precision of this method of reconstruction is comparable with that of methods applicable only for symmetric systems. The method is much more sensitive to the measurement errors because it involves the solution of an ill-conditioned problem. Traditional methods of data regularization systematically over-smooth the solution. On the grounds that an unknown systematic error is much worse than a random error, we under-smooth noisy data and then average the results of several experiments. This allows us to perform *a posteriori* error analysis and to determine the confidence intervals. For a given experimental noise level, there is a natural limit on the precision of determination of the value of the refractive index. This is not a serious concern at the moment because the experimental errors in determining boundary conditions are estimated to be of the same order of magnitude.¹⁷ Our studies elucidated the level of experimental accuracy that any measurement should attempt to achieve.

Because ray-tracing analysis is independent of the geometry of an optical system, it can be applied to a variety of problems. It requires neither an index match between the system and surrounding media nor a constant index mismatch on the boundary. The method is stable with respect to the errors in

boundary conditions. In a forthcoming paper we will discuss the application of ray-tracing analysis to the reconstruction of three-dimensional refractive index with cylindrical symmetry.

Appendix A

The deduction of the Eq. (3) from Eq. (2) is straightforward. Because

$$ds^2 = dx^2 + dy^2,$$

$$\frac{d\bullet}{ds} = \frac{d\bullet}{dx} \frac{dx}{ds} = \frac{d\bullet}{dx} \left[1 + \left(\frac{dy}{dx} \right)^2 \right]^{-1/2},$$

$$\frac{d^2\bullet}{ds^2} = \frac{d^2\bullet}{dx^2} \left[1 + \left(\frac{dy}{dx} \right)^2 \right]^{-1}.$$

Then, we write Eq. (2) in scalar form:

$$\begin{cases} \frac{dn}{dx} \left(\frac{dx}{ds} \right)^2 = \frac{\partial n}{\partial x}, \\ \frac{dn}{dx} \frac{dx}{ds} \frac{dy}{ds} + n \frac{d^2y}{dx^2} \left[1 + \left(\frac{dy}{dx} \right)^2 \right]^{-1} = \frac{\partial n}{\partial y}. \end{cases}$$

From the first equation,

$$\frac{dn}{dx} = [1 + (y')^2] \frac{\partial n}{\partial x}.$$

Substituting this in the second equation, one readily obtains

$$\frac{\partial n}{\partial x} y' + n y'' (1 + (y')^2)^{-1} = \frac{\partial n}{\partial y},$$

which is Eq. (3).

References

1. P. L. Chu, "Nondestructive measurement of index profile of an optical-fiber preform," *Electron. Lett.* **13**, 736–738 (1977).
2. P. L. Chu, "Nondestructive refractive-index profile measurement of elliptical optical fibre or preform," *Electron. Lett.* **15**, 357–358 (1979).
3. P. L. Chu and T. Whitbread, "Nondestructive determination of refractive index profile of an optical fiber: fast Fourier transform method," *Appl. Opt.* **18**, 1117–1122 (1979).
4. J. A. Ferrari, E. Frins, A. Rondoni, and G. Montaldo, "Retrieval algorithm for refractive-index profile of fibers from transverse interferograms," *Opt. Commun.* **117**, 25–30 (1995).
5. J. Sochacki, M. Sochacka, and C. Gomez-Reino, "Reconstruction of the axisymmetric refractive-index profiles from transverse interferograms in the presence of the immersion-air separating window," *J. Opt. Soc. Am. A* **7**, 211–215 (1990).
6. G. Beliaikov, "Study of the mathematical model of the refractive-index reconstruction of a smooth thin film waveguide by ray tracing," Ph.D. dissertation (People's Friendship University of Russia, Moscow, 1992) (in Russian).
7. G. Beliaikov, "Reconstruction of optical characteristics of waveguide lenses by the use of ray tracing," *Appl. Opt.* **33**, 3401–3404 (1994).
8. D. Y. C. Chan, J. P. Ennis, B. K. Pierscionek, and G. Smith, "Determination and modeling of the 3-D gradient refractive indices in crystalline lenses," *Appl. Opt.* **27**, 926–931 (1988).
9. I. H. Lira, "Reconstruction of an axisymmetric refractive index distribution with non-negligible refraction," *Meas. Sci. Technol.* **5**, 226–232 (1994).
10. C. M. Vest, "Tomography for properties of materials that bend rays: a tutorial," *Appl. Opt.* **24**, 4089–4094 (1985).
11. O. Sasaki and T. Kobayashi, "Beam-deflection optical tomography of the refractive-index distribution based on the Rytov approximation," *Appl. Opt.* **32**, 746–751 (1993).
12. O. Pomerantzeff, M. Pankratov, G.-J. Wang, and P. Dufault, "Wide-angle optical model of the eye," *Am. J. Optom. Physiol. Opt.* **61**, 166–176 (1984).
13. M. Born and E. Wolf, *Principles of Optics*, (Pergamon, Oxford, UK, 1986), p. 114.
14. Yu. A. Kravtsov and Yu. I. Orlov, *Geometrical Optics of Inhomogeneous Media*, (Springer-Verlag, Heidelberg, 1990), p. 41.
15. G. Beliaikov, "Numerical evaluation of the Luneburg's integral and ray tracing," *Appl. Opt.* **25**, 1011–1014 (1996).
16. A. L. Mikaelian, "Self-focusing media with variable index of refraction," *Prog. Opt.* **17**, 279–345 (1980).
17. B. K. Pierscionek, "Surface refractive index of the eye lens determined with an optical fiber sensor," *J. Opt. Soc. Am. A* **10**, 1867–1870 (1993).
18. P. Craven and G. Wahba, "Smoothing noisy data with spline functions," *Numer. Math.* **31**, 377–403 (1979).
19. P. Dierckx, *Curve and Surface Fitting with Splines* (Oxford U. Press, New York, 1993), p. 82.